AIAA SciTech Forum
8–12 January 2018, Kissimmee, Florida
2018 AIAA/ASCE/AHS/ASC Structures, Structural Dynamics, and Materials Conference

10.2514/6.2018-1907

# Aerodynamic Design Exploration through Point-By-Point Pareto Set Identification with Local Surrogate Models

Anand Amrit[1], and Leifur Leifsson[2]
*Computational Design Laboratory, Iowa State University, Ames, Iowa 50011*

Slawomir Koziel[3]
*Engineering Optimization & Modeling Center, Reykjavik University, Menntavegur 1, 101 Reykjavik, Iceland*



**Aerodynamic design is inherently a multi-objective problem. Obtaining the best possible trade-offs between various aerodynamic objectives can be computationally expensive when only high-fidelity computational fluid dynamics (CFD) simulations are utilized. In this work, aerodynamic design exploration is performed using a unique and computationally cheap methodology. The best-possible designs near the single-objective (SO) optimal design are determined using point-by-point exploration. This is performed using a trust-region-based multi-fidelity optimization algorithm with locally constructed response surface approximations (RSAs). In this work, the RSAs are constructed using second order polynomials without mixed terms, multi-fidelity models, and adaptive corrections. The algorithm is applied on a two-dimensional benchmark aerodynamic design case involving lift-constrained drag minimization and pitching moment minimization in inviscid transonic flow. The Pareto front is obtained at a cost of few evaluations of the high-fidelity CFD model. At the end, it is clearly shown how point-by-point can be a fast method to obtain Pareto or part of the Pareto for problems involving physics based simulations.**

## Nomenclature

| | | |
|---|---|---|
| $A$ | = | cross-sectional area |
| $C_d$ | = | drag coefficient |
| $C_m$ | = | pitching moment coefficient |
| $C_l$ | = | lift coefficient |
| **c** | = | low-fidelity model |
| $c$ | = | chord length |
| **f** | = | high-fidelity model |
| **l** | = | lower bounds vector |
| $M_\infty$ | = | Mach number |
| **u** | = | upper bounds vector |
| **x** | = | design variable vector |

***Abbreviations***

| | | |
|---|---|---|
| cts | = | counts |
| MOO | = | multi-objective optimization |
| RSA | = | response surface approximation |
| SBO | = | surrogate-based optimization |
| SOO | = | single-objective optimization |
| SM | = | space mapping |

[1] Graduate Student, Department of Aerospace Engineering, Student Member AIAA.
[2] Assistant Professor, Department of Aerospace Engineering, Senior Member AIAA.
[3] Professor, School of Science and Engineering, Senior Member AIAA.

## I. Introduction

Multi-objective optimization has become a vital step in the design of aerodynamic surfaces, such as aircraft wings and turbine blades.[1,2] An evaluation of the system is most commonly obtained by means of high-fidelity computational fluid dynamic (CFD) simulations as the results are close to that of experimental results. This helps in automation of the design process along with substantial reduction of cost because of the reduced number of prototyping steps and physical measurements involved in the process. Nevertheless, simulation-driven design is still often based on interactive methods such as CFD-based parameter sweeps guided by engineering experience. Design automation using multi-objective optimization techniques is highly desirable and is becoming more and more popular[3-6] where decisions need to be taken among numerous conflicting objectives. A variety of techniques have been utilized for multi-objective aerodynamic shape optimization, such as gradient-based methods[7-9], and surrogate-based optimization (SBO) techniques[10-15]. A vital advantage of SBO compared to conventional algorithms, is the possibility of efficient global optimization (by using data-driven surrogates), and a considerable reduction of the design cost as compared to traditional method, which is particularly the case for methods exploiting multi-fidelity methods.[12]

Handling multiple criteria is a necessary challenge of practical aerodynamic shape optimization problems. When considering only the aerodynamics, the typical design objectives include drag minimization, lift maximization, and a reduction of the aero-acoustic noise. A rudimentary approach to simultaneous control of several criteria is an a priori preference articulation (i.e., selection of the primary objective such as drag minimization) and handling the remaining objectives by means of constraints of penalty functions. Such a problem can be solved as a single-objective one. However, in some situations it is of interest to gain more comprehensive information about the system at hand which may allow the designer to understand the characteristics of possible trade-offs between conflicting objectives. Moreover, other disciplines come into play when doing design, such as the structures. In such cases, a genuine multi-objective optimization is necessary.

The subject of this paper involves finding strategies to efficiently determine the possible trade-offs in a given system when aerodynamics is one of them. In this work, however, we will restrict the system to contain only the aerodynamic surfaces. This is done to simplify these initial investigations. Future work will account for interactions with other complex systems. More specifically, here we attempt to solve a two-dimensional airfoil shape design case by utilizing variable-resolution CFD simulation models in combination with an optimization method known as point-by-point Pareto set identification method, originally developed in the field of microwave engineering[16], for expedited multi-objective aerodynamic design optimization. Using this method, we reach one end of the Pareto front and then travel along the Pareto front point by point. A local response surface approximation (RSA) model is built around the extreme point and a local optimum search is performed to hunt the nearest point in the Pareto.

## II. Multi-Objective Optimization Methodology

This section describes the aerodynamic shape optimization problem formulation, and the multi-objective optimization procedure.

### A. Formulation of the Multi-Objective Problem

Let $\mathbf{x}$ be the $n$ x 1 vector of $n$ design variables. Let $\mathbf{f}(\mathbf{x}) = [C_{l.f}(\mathbf{x})\ C_{d.f}(\mathbf{x})\ C_{m.f}(\mathbf{x})]^T$ be the attributes of the airfoil obtained by an accurate high-fidelity aerodynamics simulation model. Here, the scalars $C_{l.f}$, $C_{d.f}$, and $C_{m.f}$ are the lift, drag, and pitching moment coefficients, respectively. Let $F_k(\mathbf{x})$, $k = 1, \ldots, N_{obj}$, be a $k$th design objective of interest. A typical performance objective would be to minimize the drag coefficient, in which case $F_k(\mathbf{x}) = C_{d.f}$. Another objective would be to minimize the pitching moment coefficient, i.e., $F_k(\mathbf{x}) = C_{m.f}$.

If $N_{obj} > 1$ then any two designs $\mathbf{x}^{(1)}$ and $\mathbf{x}^{(2)}$ for which $F_k(\mathbf{x}^{(1)}) < F_k(\mathbf{x}^{(2)})$ and $F_l(\mathbf{x}^{(2)}) < F_l(\mathbf{x}^{(1)})$ for at least one pair $k \neq l$, are not commensurable, i.e., none is better than the other in the multi-objective sense. We define Pareto dominance relation $\prec$ (see, e.g., Fonseca[16]), saying that for the two designs $\mathbf{x}$ and $\mathbf{y}$, we have $\mathbf{x} \prec \mathbf{y}$ ($\mathbf{x}$ dominates $\mathbf{y}$) if $F_k(\mathbf{x}) < F_k(\mathbf{y})$ for all $k = 1, \ldots, N_{obj}$. The goal of the multi-objective optimization if to find a representation of a so-called Pareto front (of Pareto-optimal set) $\mathbf{X}_P$ of the design space $\mathbf{X}$, such that for any $\mathbf{x} \in \mathbf{X}_P$, there is no $\mathbf{y} \in \mathbf{X}$ for which $\mathbf{y} \prec \mathbf{x}$ (Fonseca[16]).

### B. Multi-Objective Optimization Algorithm

The multi-objective optimization (MOO) algorithm is formulated in terms of two scalar design objectives, $F_1$ and $F_2$. Initially, a point on the Pareto front is obtained to be used as the starting point for Pareto front exploration. A single objective optimization is carried out for one of the objective function while subjecting the second objective function

into a non-linear constraint. The MOO algorithm produces a sequence of designs $\mathbf{x}^{(k)}$, k = 1,2,…, is produced where $\mathbf{x}^{(1)}$ is a solution to the single-objective optimization problem of the form

$$\mathbf{x}^{(1)} = \arg \min_{\mathbf{x}} F_1(\mathbf{f}(\mathbf{x})), \tag{1}$$

subjected to

$$F_2(\mathbf{f}(\mathbf{x})) - b \leq 0 \text{ or } F_2(\mathbf{f}(\mathbf{x})) - b \geq 0,$$

where $b$ is the threshold value for the second objective. Thus, an optimum design value of the first objective is obtained which lies in the mid of Pareto front, to be explored.

To improve the computational efficiency, the method exploits a combination of the accurate high-fidelity model **f**, and a model **c**, which is of lower fidelity than **f** but is computationally faster to evaluate. In this work, the low-fidelity model **c** is based on coarse-discretization CFD simulations. Solution to (1) is obtained using single-objective surrogate-based optimization (SOSO) with the low fidelity model **c** and output space mapping as a space mapping model correction method[12].

Further, succeeding designs along the Pareto are obtained by exploring it point-by-point. The optimal design from solution (1) is utilized as a starting point and a constrained single objective optimization is performed to get the next point in the Pareto. Let $F_2^{(k)}$ be the threshold value for the second objective, then we have

$$\mathbf{x}^{(k)} = \arg \min_{\mathbf{x}, F_2(\mathbf{f}(\mathbf{x})) \leq F_2^{(k)}} F_1(\mathbf{f}(\mathbf{x})). \tag{2}$$

Here, $\mathbf{x}^{(k)}$ is the kth element of the Pareto set and the process is continued until the design specifications are met. Points can be obtained in both directions along the Pareto, i.e., above and below the optimal design from solution (1). To obtain the Pareto above the starting point, the problem formulation is as follows:

$$\min_{l \leq x \leq u} F_1, \ \max_{l \leq x \leq u} F_2. \tag{3}$$

subject to $h(x) = 0$, and $g(x) \leq 0$.

### C. Pareto Front Exploration Using Local Response Surface Approximation Models

Search for a point $\mathbf{x}^{(k)}$ close to the design $\mathbf{x}^{(k-1)}$ is performed and is obtained iteratively as a sequence of $\mathbf{x}^{(k,j)}$, j = 0, 1, …, with $\mathbf{x}^{(k,0)} = \mathbf{x}^{(k-1)}$, as follows

$$\mathbf{x}^{(k,j+1)} = \arg \min_{\mathbf{x}, F_2(\mathbf{s}(\mathbf{x})) \leq F_2^{(k)}} F_1(\mathbf{s}^{(k,j)}(\mathbf{x})), \tag{4}$$

where the surrogate $\mathbf{s}^{(k,j)}$ is defined as

$$\mathbf{s}^{(k,j)}(\mathbf{x}) = \mathbf{s}_q^{(k,j)}(\mathbf{x}) + [\, \mathbf{f}(\mathbf{x}^{(k,j)}) - \mathbf{s}_q^{(k,j)}(\mathbf{x}^{(k,j)}) \,], \tag{5}$$

where $\mathbf{s}_q^{(k,j)}$ is a local response surface approximation (RSA) model of **c**, constructed in the vicinity of current design $\mathbf{x}^{(k,j)}$. Equation (5) is solved in the vicinity $[\mathbf{x}^{(k,j)} - \mathbf{d}, \mathbf{x}^{(k,j)} + \mathbf{d}]$, where **d** is the size vector. The RSA model $\mathbf{s}_q$ is a quadratic model without mixed terms and is constructed using few evaluations.

The multi-objective design optimization algorithm is summarized as follows:

1. Obtain $\mathbf{x}^{(1)}$ by performing single objective surrogate based optimization;
2. Set $F_2^{(1)} = F_2(\mathbf{f}(\mathbf{x}^{(1)}))$ and set $k = 2$;
3. Set $\mathbf{x}^{(k,0)} = \mathbf{x}^{(k-1)}$;
4. Evaluate $\mathbf{f}^{(k,j)}(\mathbf{x}^{(k,j)})$;
5. Construct local RSA model $\mathbf{s}_q^{(k,j)}(\mathbf{x})$ within the range region defined as $[\mathbf{x}^{(k,j)} - \mathbf{d}, \mathbf{x}^{(k,j)} + \mathbf{d}]$;
6. Use (3) to obtain $\mathbf{x}^{(k,j+1)}$ by optimizing surrogate model $\mathbf{s}_q^{(k,j)}(\mathbf{x})$;
7. If j = 2 set $\mathbf{x}^{(k)} = \mathbf{x}^{(k,j+1)}$ and go to Step 8; else set $\mathbf{d} = \mathbf{d}/\mathbf{m}$, set $j = j + 1$ and go to Step 4;
8. If termination condition is met end algorithm; otherwise set $k = k+1$, set threshold $F_2^{(k)}$ and go to Step 3.

## III. Numerical Example

### A. Problem Formulation

The objective is to find the trade-offs between the conflicting objectives, drag coefficient ($C_d$) and pitching moment coefficient ($C_m$) of the RAE 2822 at a free-stream Mach number of $M_\infty = 0.734$, a constant lift coefficient of 0.824, and Reynolds number of $6.5 \times 10^6$, subject to an area and pitching moment constraint. We want to explore the designs in both feasible and infeasible regions while satisfying the area constraint at a constant lift coefficient. The conflicting objectives considered here are: drag minimization and pitching moment minimization, i.e., we have $F_1(\boldsymbol{x}) = C_{d.f}$ and $F_2(\boldsymbol{x}) = C_{m.f}$.

The problem formulation is written as follows

$$\min_{l \le x \le u} C_d, \ \max_{l \le x \le u} C_m \tag{6}$$

subject to

$$C_l = 0.824, \tag{7}$$

$$C_m \ge -0.092, \tag{8}$$

$$A \ge A_{baseline}. \tag{9}$$

### B. Design Variables

The B-spline parameterization approach, described in Jie *et al.*[17], is used in this case to control the upper and lower surfaces of the airfoil. We use eight control points, as shown in Fig. 1(a), where two are fixed at the leading- and trailing-edges, and the other ones, four for each surface, can move in the vertical direction. Based on a fit to the RAE2822, we set the $x/c$-locations of the free control points as: $\mathbf{X} = [\mathbf{X}_u; \mathbf{X}_l]^T$ = [0.0 0.15 0.45 0.80; 0.0 0.35 0.60 0.90]$^T$. The initial design variable vector is $\mathbf{x} = [\mathbf{x}_u; \mathbf{x}_l]^T$ = [0.0175 0.0498 0.0688 0.0406; -0.0291 -0.0679 -0.0384 0.0054 ]$^T$. The lower bound of $\mathbf{x}$ is set as $\mathbf{l}$ = [0.015 0.015 0.015 0.015; -0.08 -0.08 -0.08 -0.01]$^T$, and the upper bound is set as $\mathbf{u}$ = [0.08 0.08 0.08 0.08;-0.01 -0.015 -0.015 0.01]$^T$.

### B. High-Fidelity Viscous Aerodynamics Model (f)

The SU$^2$ implicit density-based flow solver is used for the viscous case, solving the steady compressible Reynolds-averaged Navier-Stokes (RANS) equations with the Spalart-Allmaras turbulent model[18]. The convective flux will be calculated using the second order JST scheme[19]. One multi-grid level is used for solution acceleration. The turbulent variables are convected using a first-order scalar upwind method. The flow solver convergence criterion is the one that occurs first of the two: (i) the change in the drag coefficient value over the last 100 iterations is less than $10^{-5}$, or (ii) a maximum number of iterations of 20,000 is met.

The grids are generated using the hyperbolic C-mesh of Kinsey and Barth[20] (see Fig. 1(b)). The farfield is set 100 chords away from the airfoil surface. The grid points are clustered at the trailing edge and the leading edge of the airfoil to give a minimum streamwise spacing of $0.001c$, and the distance from the airfoil surface to the fist node is $10^{-5}c$. The grid density is controlled by the number of points in the streamwise direction, and the number of points in the direction normal to airfoil surface. We set the number of points in the wake region equal to the number in the normal direction. Table 1 gives the results of a grid convergence study using the RAE 2822 airfoil at $M = 0.734$ and $C_l = 0.824$. The constant lift condition is determined by internally changing the angle of attack within the flow solver. The simulation time presented in Table 1 gives the overall time to compute the constant lift condition.

For the optimization studies, we use Mesh 3 for the high-fidelity model **f**. Mesh 4 is the finest and the most accurate. The difference between meshes 3 and 4 is around 1.75 drag counts for the baseline shape. However, Mesh 4 is almost five times more expensive than Mesh 3, hence the latter was chosen as the high-fidelity model for this work.

### C. Low-Fidelity Viscous Aerodynamics Model (c)

The model set up for low-fidelity model is same as that of high-fidelity model (**f**). As shown in Table 1, we use Mesh 1 for the low-fidelity model **c**. The low-fidelity model convergence criteria are set with the following values: (i) change in the drag coefficient value over the last 100 iterations is less than $10^{-4}$, or (ii) the maximum number of iterations is set to 5,000. The low-fidelity solver is converged well within 5,000-iteration limit, and is a good representation of high-fidelity one in terms of the pressure coefficient distributions.

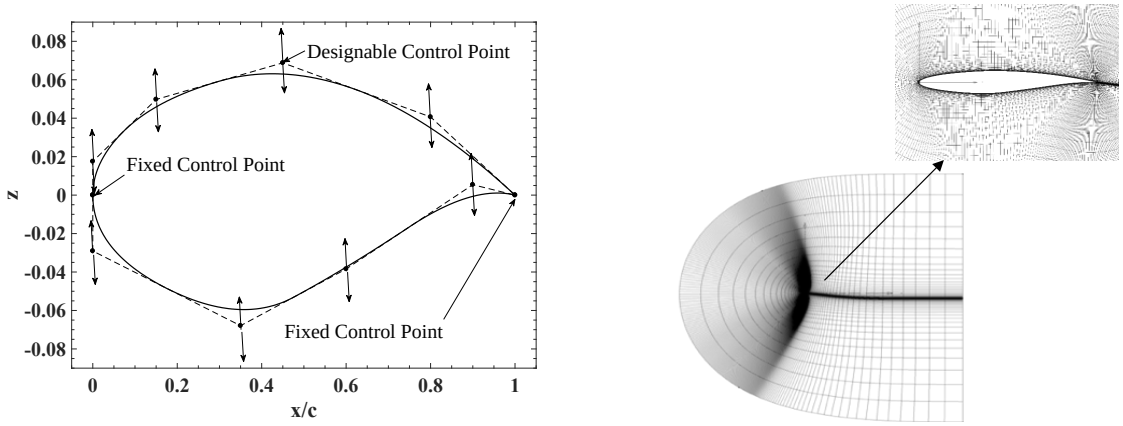


**(a)** **(b)**

**Figure 1. Aerodynamic modeling: (a) airfoil shape parameterization using B-spline curves for the upper and lower surfaces. (b) hyperbolic C-mesh used in the viscous model: farfield view and view close to surface**

**Table 1. Grid convergence study for the baseline shape of Benchmark Case 2.**

| Mesh | Number of Elements | Lift Counts (l.c.) | Drag Counts (d.c.) | Simulation Time* (min) |
|---|---|---|---|---|
| 1 | 9,836 | 0.824 | 324.6 | 3.1 |
| 2 | 38,876 | 0.824 | 221.5 | 8.8 |
| 3 | 154,556 | 0.824 | 204.8 | 34.0 |
| 4 | 616,316 | 0.824 | 203.0 | 152.6 |

* Computed on a high-performance cluster with 32 processors. Flow solution only.

### C. Single-Objective Optimization (SOO) Results

The SOO problem is solved using space mapping (SM) algorithm[12]. Figure 2(a) and 2(b) show the convergence history of the algorithm indicating a considerable reduction in the objective function compared to that of the baseline airfoil. As can be seen in Table 2, the SM algorithm reduces the drag coefficient value from 203.80 cts to 119.49 cts. Figures 2(c) and 2(d) show comparisons of the shapes and pressure coefficient distributions of the baseline and SOO optimal designs. Figures 2(e) and 2(f) show the pressure coefficient contours of the baseline and optimum shape design respectively, indicating a considerable reduction of shock strength. In terms of number of function evaluations, SM based optimization utilized 499 low fidelity models and only 4 high fidelity models. The cost in terms of CPU time for the entire optimization process is approximately 19 hours on a HPC with 32 processors.

### D. Pareto Front Exploration Results

The Pareto front exploration in feasible and infeasible regions is performed using algorithm described in section II. The initial design corresponding to the best possible value of the first objective (minimum drag coefficient) is obtained in the first step of the process using space mapping (SM) algorithm[12]. A target pitching moment value is then identified for the algorithm to attain while minimizing drag coefficient value. The runs are performed at $M_\infty = 0.734$ and $A_{\text{baseline}} = 0.0779$. Subsequent designs along the Pareto were obtained using (2) and the process is terminated when the target pitching moment value reaches approximately +/- 25% of the pitching moment for initial design. The proposed algorithm needed one iteration to reach each target point. The cost of stepping from one point to another is approximately one hour. The total cost in terms of CPU time to obtain the entire Pareto is around 30 hrs on a HPC with 32 processors which includes cost of obtaining the initial design.

Figures 3(a) and (b) show the optimal solution set (Pareto front) obtained and a zoomed-in plot near SOO optimum respectively. The plots clearly reflect that; we cannot obtain any better optimum drag coefficient value other than SOO optimum. Few points (Point 1 and point 2) on the Pareto optimal set were selected to be compared with SOO optimum and the baseline design. Figures 3(c) and (d) show comparisons of all the airfoil shape designs and the pressure coefficient distributions for the selected points. There is not much difference in the pressure coefficient distribution compared to that of SOO optimum and that's because the selected points are near the optimum drag coefficient value.

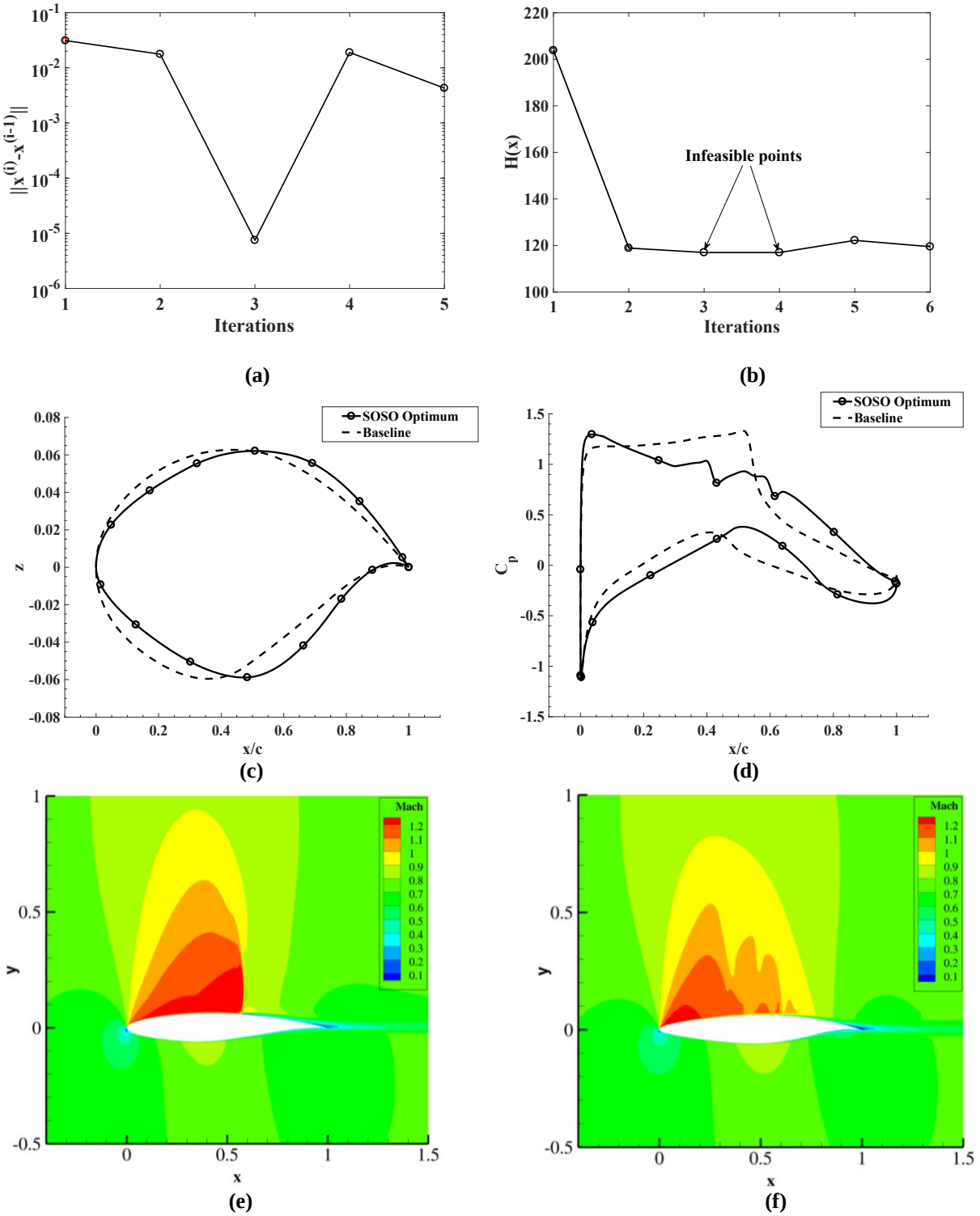


**Figure 2. Single-objective optimization results: (a) convergence history of the arguments, (b) evolution of the objective function, (c) airfoil shape comparison, (d) pressure distribution comparison, (e) pressure coefficient contours of baseline airfoil, (f) pressure coefficient contours of optimum design from SOO.**

**Table 2. Single objective optimization results**

| Parameter/method | Baseline | SOO |
|---|---|---|
| $C_l$ (l.c.) | 82.4 | 82.4 |
| $C_d$ (d.c.) | 203.8 | 118.4 |
| $C_{m,c/4}$ | -0.0905 | -0.0904 |
| $A$ | 0.0779 | 0.0779 |
| $N_c$ | - | 499 |
| $N_f$ | - | 4 |
| CPU Time (hours) | - | 13.55 |

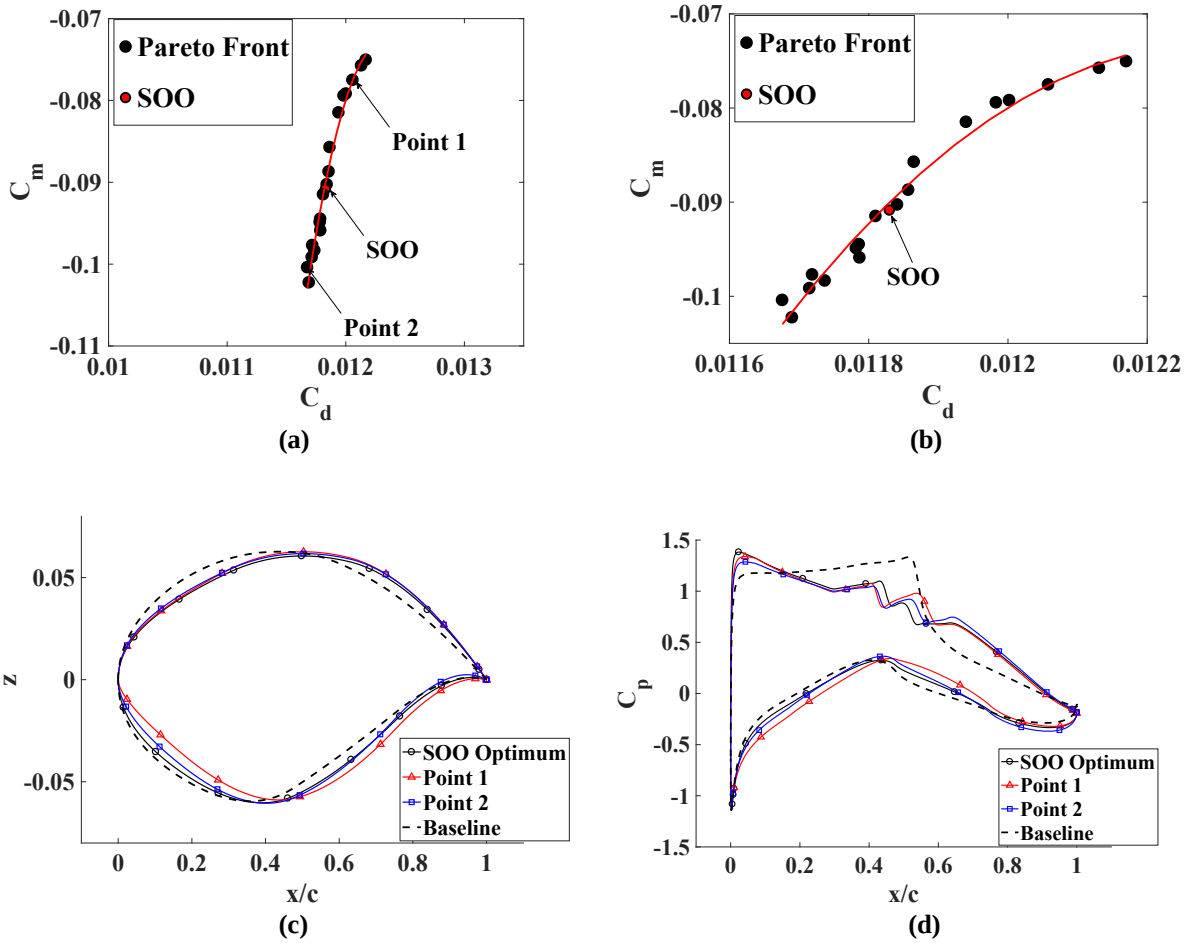


**Figure 3. Multi-objective optimization results: (a) optimum solution set in feasible and infeasible regions, (b) zoomed-in plot of Fig. 3(a), (c) pressure distribution comparison, and (d) airfoil shape comparison.**

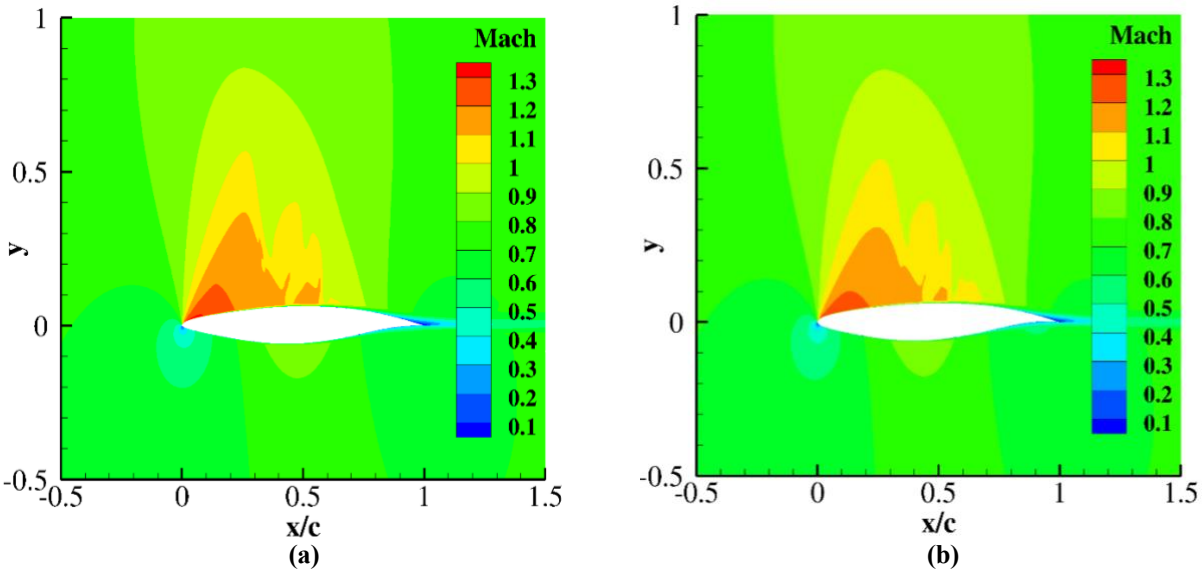


**Figure 4. Pressure Coefficient Contours of (a) Point 1, (b) Point 2.**

## IV. Conclusion

An efficient methodology for aerodynamic design exploration is proposed in this paper using point-by-point Pareto set identification and local surrogate models. In particular, the approach yields the best possible trade-offs between conflicting objectives using a combination of local approximation-based surrogates and multi-fidelity models at each to determine target points on the Pareto front in the vicinity of a single-objective optimal design. The approach was demonstrated on a two-dimensional transonic airfoil design problem within a small design space. The overall cost of determining the Pareto front is low. Future work will consider the generalization of the proposed method that could handle larger number of design variables and conflicting objectives.

## References

[1]Leoviriyakit, K., Kim, S., and Jameson, A., "Viscous Aerodynamic Shape Optimization of Wings including Planform Variables," *21st Applied Aerodynamics Conference*, Orlando, Florida, June 23-26, 2003.

[2]Braembussche, R.A., "Numerical Optimization for Advanced Turbomachinery Design," In *Optimization and Computational Fluid Dynamics*, Thevenin, D. and Janiga, G., editors, Springer, 2008, pp. 147-189.

[3]Mader, C. A., and Martins, J. R. R. A., "Derivatives for Time-Spectral Computational Fluid Dynamics Using an Automatic Differentiation Adjoint," *AIAA Journal*, Vol. 50, No. 12, 2012, pp. 2809-2819.

[4]Mousavi, A., and Nadarajah, S., "Heat Transfer Optimization of Gas Turbine Blades Using an Adjoint Approach," *13th AIAA/ISSMO Multidisciplinary Analysis Optimization Conference*, AIAA Paper 2010-9048, Fort Worth, Texas, Sept. 13-15, 2010.

[5]Leung, T.M., and Zingg, D.W., "Aerodynamic Shape Optimization of Wings Using a Parallel Newton-Krylov Approach," *AIAA Journal*, Vol. 50, No. 3, 2012, pp. 540-550.

[6]Epstein, B., and Peigin, S., "Constrained Aerodynamic Optimization of Three-Dimensional Wings Driven by Navier-Stokes Computations", *AIAA Journal*, Vol. 43, No. 9, 2005, pp. 1946-1957.

[7]Nocedal, J., and Wright, S.J., *Numerical Optimization*, Springer, 2006.

[8]Kim, S., Hosseini, K., Leoviriyakit, K., and Jameson, A., "Enhancement of Class of Adjoint Design Methods via Optimization of Parameters", *AIAA Journal*, Vol. 48, No. 6, 2010, pp. 1072-1076.

[9]Schmidt, S., Gauger, N., Ilic, C., and Schulz, V., "Three Dimensional Large Scale Aerodynamic Shape Optimization based on Shape Calculus", *41st AIAA Fluid Dynamics Conference and Exhibit*, AIAA Paper 2011-3718, Honolulu, Hawaii, June 27-30, 2011.

[10]Queipo, N.V., Haftka, R.T., Shyy, W., Goel, T., Vaidyanathan, R., and Tucker, P.K., "Surrogate-Based Analysis and Optimization," *Progress in Aerospace Sciences*, Vol. 41, No. 1, 2005, pp. 1-28

[11]Forrester, A.I.J., and Keane, A.J., "Recent advances in surrogate-based optimization," *Progress in Aerospace Sciences*, Vol. 45, No. 1-3, 2009, pp. 50-79.

[12]Koziel, S., Echeverría-Ciaurri, D., and Leifsson, L., "Surrogate-based methods," in S. Koziel and X.S. Yang (Eds.) *Computational Optimization, Methods and Algorithms*, Series: Studies in Computational Intelligence, Springer-Verlag, pp. 33-60, 2011.

[13]Alexandrov, N.M., Lewis, R.M., Gumbert, C.R., Green, L.L., and Newman, P.A., "Optimization with Variable-Fidelity Models Applied to Wing Design," *38th Aerospace Sciences Meeting & Exhibit*, Reno, NV, AIAA Paper 2000-0841, Jan. 2000.

[14]Robinson, T.D., Eldred, M.S., Willcox, K.E., and Haimes, R., "Surrogate-Based Optimization Using Multifidelity Models with Variable Parameterization and Corrected Space Mapping," *AIAA Journal*, vol. 46, no. 11, 2008.

[15]Booker, A.J., Dennis Jr., J.E., Frank, P.D., Serafini, D.B., Torczon, V., and Trosset, M.W., "A rigorous framework for optimization of expensive functions by surrogates," *Structural Optimization*, Vol. 17, No. 1, 1999, pp. 1-13.

[16]Koziel, S., Bekasiewicz, A., "Rapid Multi-Objective Antenna Design Using Point-By-Point Pareto Set Identification," *IEEE Transactions of Antennas and Propagation*, vol. 64, no. 6, 2016.

[17]Ren, Z., Thelen, A. S., Amrit, A., Du, X., Leifsson, L., Tesfahunegn, Y.A., Koziel, S., "Application of Multifidelity Optimization Techniques to Benchmark Aerodynamic Design Problems", *54th AIAA Aerospace Sciences Meeting*, San Diego, California, USA.

[18]Spalart, P. R. and Allmaras, S. R., "A One Equation Turbulence Model for Aerodynamic Flows", AIAA-Paper-92-0439, *38th AIAA Aerospace Sciences Meeting and Exhibit*, Reno, NV, January 6-9, 1992.

[19]Jameson, A., Schmidt, W., and Turkel, E., "Numerical Solution of the Euler Equations by Finite Volume Methods Using Runge-Kutta Time-Stepping Schemes," AIAA 1981-1259, *AIAA 14th Fluid and Plasma Dynamic Conference*, Palo Alto, CA, June 23-25, 1981.

[20]Kinsey, D. W., and Barth, T. J., "Description of a Hyperbolic Grid Generation Procedure for Arbitrary Two-Dimensional Bodies," AFWAL TM 84-191-FIMM, 1984.